Review

Nitrogen-Related Defects in Crystalline Silicon

E. N. Sgourou [1], N. Sarlis [1], A. Chroneos [2,3,*] and C. A. Londos [1]

1   Section of Condensed Matter Physics, Department of Physics, National and Kapodistrian University of Athens, Panepistimiopolis Zografos, 15784 Athens, Greece; e_sgourou@hotmail.com (E.N.S.); nsarlis@phys.uoa.gr (N.S.); hlontos@gmail.com (C.A.L.)
2   Department of Electrical and Computer Engineering, University of Thessaly, 38333 Volos, Greece
3   Department of Materials, Imperial College London, London SW7 2BP, UK
*   Correspondence: alexander.chroneos@imperial.ac.uk; Tel.: +30-6978775320

Abstract: Defects and impurities play a fundamental role in semiconductors affecting their mechanical, optical, and electronic properties. Nitrogen (N) impurities are almost always present in a silicon (Si) lattice, either unintentionally, due to the growth and processing procedures, or intentionally, as a result of implantation. Nitrogen forms complexes with intrinsic defects (i.e., vacancies and self-interstitials) as well as with other impurities present in the Si lattice such as oxygen and carbon. It is, therefore, necessary to investigate and understand nitrogen-related defects, especially their structures, their energies, and their interaction with intrinsic point defects and impurities. The present review is focused on nitrogen-related defects (for example N_i, N_s, N_iN_i, N_iN_s, N_sN_s); nitrogen–self-interstitial and nitrogen-vacancy-related complexes (for example N_sV, $(N_iN_i)Si_i$, $(N_sN_s)V$); nitrogen–oxygen defects (for example NO, NO_2, N_2O, N_2O_2); more extended clusters such as $V_mN_2O_n$ (m, n = 1, 2); and nitrogen–carbon defects (for example C_iN and C_iNO). Both experimental and theoretical investigations are considered as they provide complementary information.

Keywords: silicon; nitrogen; intrinsic defects

1. Introduction

Si has been a dominant material in the semiconductor industry for over six decades. It has a wide range of applications in electronic, microelecronic, and optoelectronic fields and especially for nanoelectronic, nuclear medicine, and sensor and photovoltaic devices [1–5]. Typically, Si-based devices are fabricated on single-crystal Czochralski Si wafers. Importantly, all semiconductors contain defects, mostly impurities and lattice defects, which are introduced either during crystal growth and material processing or on purpose and by design for certain applications. The performance of Si-based devices is directly related to the properties of the defects present in the lattice. The technological necessity to improve the quality of Si to sustain and enhance the device efficiency depends on the control of the defects present in the lattice [6–8].

N is one of the fundamental impurities incorporated in the Si lattice and has attracted a lot of attention in the last 50 years [9–14]. It is introduced in Si either during material processing in a nitrogen atmosphere or through implantation [9]. There is intensive research on the impact of N in Si, since it affects the properties of the material in many ways. It has been found that N introduction into Si enhances the mechanical strength of the wafers, thus obstructing the movement of dislocations during thermal treatments [11,15,16]. It also enhances oxygen precipitation, which is important for internal gettering as it suppresses the effect of deleterious metal contaminants [13,17]. It also suppresses self-interstitial diffusion and controls the density and size of crystal-originated particles (COPs) [11–13,18], thus improving dramatically the gate oxide integrality of semiconductor devices. It suppresses void formations, which are essentially vacancy aggregates that degrade properties of the devices [12,19]. This is directly correlated with the formation of nitrogen-vacancy pairs [20].

N suppress interstitial- (A-swirl) and vacancy (D-voids)-related defects [12,21]. Generally, diffusion and/or the aggregation process of Si self-interstitials and vacancies are affected by N incorporation [22]. The N-suppression effect on the as-grown defects in Si is very suitable for the fabrication of insulated gate bipolar transistors (IGBTs) which have attracted considerable attention for their potential use in the electric vehicle industry [23]. There is experimental evidence that N implantation in Si induces transient enhanced diffusion of dopants [24]. N can suppress the effect of deleterious defects in Si, for instance of substitutional Au impurities, by reducing their concentration [25]. It has been determined that the pulling rate range of defect-free crystal is wider in N-doped Cz-Si, which is a key issue in Si technology [26]. It has also been reported that N incorporation in Cz-Si has no significant effect on the denuded zone of the crystal which can satisfy the requirements of the microelectronic industry [27]. Importantly, N in Cz-Si reduces high-purity-argon consumption during processing which in turn reduces the cost of Si crystal growth [13].

N incorporation in the Si lattice is, therefore, very important for the improvement of the efficiency of Si-based devices for certain applications. One key issue is the ability of N to form complexes with vacancies as well as with other impurities such as oxygen and carbon. Density functional theory (DFT) calculations have shown that the formation of such complexes is energetically favored [22,28,29]. The interaction of N with the above defects can lead to complexes, some of which are electrically inactive [30], and others are active, such as for instance shallow thermal donors [31]. Apparently, a better understanding of the physical properties of these N-related complexes will improve the quality of Si wafers and thus enhance the efficiency of the devices. Thus, these complexes have been studied systematically both experimentally and theoretically. Experimentally, there have been a variety of techniques employed to study defects in semiconductors and, especially in this work, N-related defects in Si: a) those studying the electrical properties of defects [32–35] use, for instance, the deep-level transient spectroscopy (DLTS) technique which basically investigates the properties of deep levels in the forbidden gap of semiconductors; b) those studying the magnetic properties of defects [32,36–38] use, for instance, the electron paramagnetic resonance technique (EPR) spectroscopy which is used to identify the electronic structure of defects and their charge states; and c) those studying the optical properties of defects use, for instance, infrared spectroscopy (IR) which mainly investigates using infrared absorption of the localized vibrational modes (LVMs) of the defects [39–43], as well as photoluminescence (PL) where light separates charge carries within the band or impurity structure of a semiconductor, and whose later recombination produce characteristic emissions [44–46].

Theoretically, a lot of works have been published employed DFT as well as semi-empirical calculations to gain insight into the structure, binding energies, electronic and vibrational properties, and the behavior of various nitrogen-related defects in Si [47–57].

In the present review, we focus on the most important nitrogen-related defects and their properties in Si. We consider both the experimental and theoretical studies on these technologically important nitrogen-related defects in Si.

2. Background Information of N-Related Defects in Si

2.1. Nitrogen Substitutional (N_s) and Interstitial (N_i) Defects

In the substitutional configuration a Si atom is substituted with a N atom. N is a Group V impurity. However, unlike the other elements of this group (phosphorous (P), arsenic (As), antimony (Sb), and bismuth (Bi)), which possess on-site T_d symmetry, N is trigonally distorted from the regular tetrahedral site preserving C_{3v} symmetry along the <111> axis, as determined using EPR measurements. An EPR signal Si-SL5 was associated with a N substitutional defect [9,36,38]. EPR studies have determined that the off-center substitutional N is more stable than the on-center substitutional N [36,58–60]. Interestingly, an argument for a metastable on-center configuration was put forward in order to explain the hyperfine splitting observed in the EPR spectra with increased temperature, and a symmetry breaking mechanism $T_d \rightarrow C_{3v}$ was proposed [32,60]. An infrared band at

653 cm^{-1} (at 300 K) was ascribed [61] to the N's substitutional impurity. Additionally, unlike the other members of the group that introduce shallow levels in the forbidden gap, N behaves as a deep-level impurity. Indeed, DLTS measurements have found that a single donor level at E_c −0.31 eV and a single acceptor level at E_c −0.08 eV should be attributed [62] to the N's substitutional impurity. Furthermore, a single acceptor level at E_c −0.64 eV and a double acceptor level at E_c −0.34 eV were also associated [33] with the N's substitutional impurity.

Recent DFT calculations by Kuganathan et al. [54] considered bonding between the N_s (refer to Figure 1a) and the Si atoms by plotting a charge density map (refer to Figure 1c). The strong N-Si bonds have, as expected, shorter N–Si bond lengths and negative Bader charge on N_s in the NSi$_4$ tetrahedral unit (refer to Figure 1b) [54]. At this point, the importance of the significantly higher electronegativity of N (3.04) as compared to Si (1.90) should be stressed. It is the reason why, in the Bader charge analysis, the N_s atom gains nearly three electrons from the nearest neighbor Si atoms (refer to Figure 1b) [54]. The band-decomposed charge density plot for N_s (refer to Figure 1d) shows the electron density more clearly [54]. In the DOS plots, the states appearing in the bandgap are primarily due to the s electrons of N_s. Accordingly, the *p*-states of N_s are localized with the lattice as they are in the valence band (refer to Figure 1e,f).
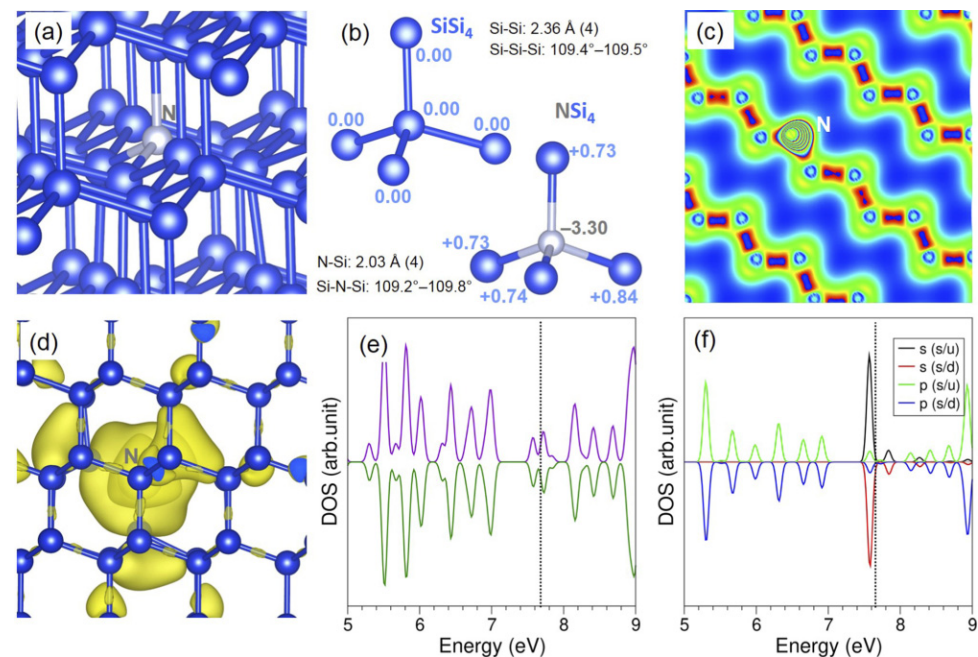
Figure 1. (**a**) The N_s in the Si lattice; (**b**) tetrahedral units comparing Bader charges, bond distances, and angles; (**c**) charge density; (**d**) band-decomposed charge density plot for N_s; (**e**) total DOS, and (**f**) atomic DOS plot of N [54].

For the N_i location within the Si lattice, several sites have been investigated theoretically, for instance, investigating the split-interstitial site, the bond center site, the hexagonal site, and the tetrahedral site (refer to Figure 2) [49–51,63]. The more stable configuration for the neutral N_i interstitial defect is a slightly distorted <001> split-interstitial site, where the ideal C_v symmetry has been lost through a slight displacement of the core Si atom along a <110> axis [50]. In this configuration, the N_i has a similar formation energy as the N_s [63]. An EPR signal labeled Si-NL26 was tentatively associated [37] with a neutral interstitial N. DFT calculations have reported [50] three LVMs of the N interstitial defect at 550, 773, and 885 cm^{-1}. Additionally, it was found [63] that the defect possesses a donor level at E_v +0.5 eV and an acceptor level at E_c −0.2 eV in agreement with other previous studies [51].
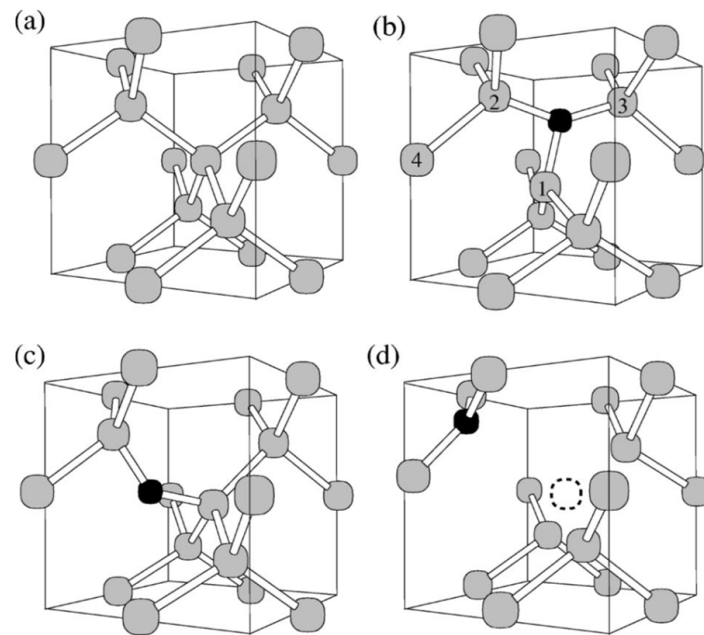
Figure 2. A schematic representation of the defects with a single nitrogen atom. (**a**) The Si lattice, (**b**) the C_{1h} <001> nitrogen split-interstitial site, (**c**) the N_i puckered bond-centered structure, and (**d**) the N_sV defect. Black and gray circles represent the N and Si atoms, whereas the vacancy is indicated with a dashed circle [50].

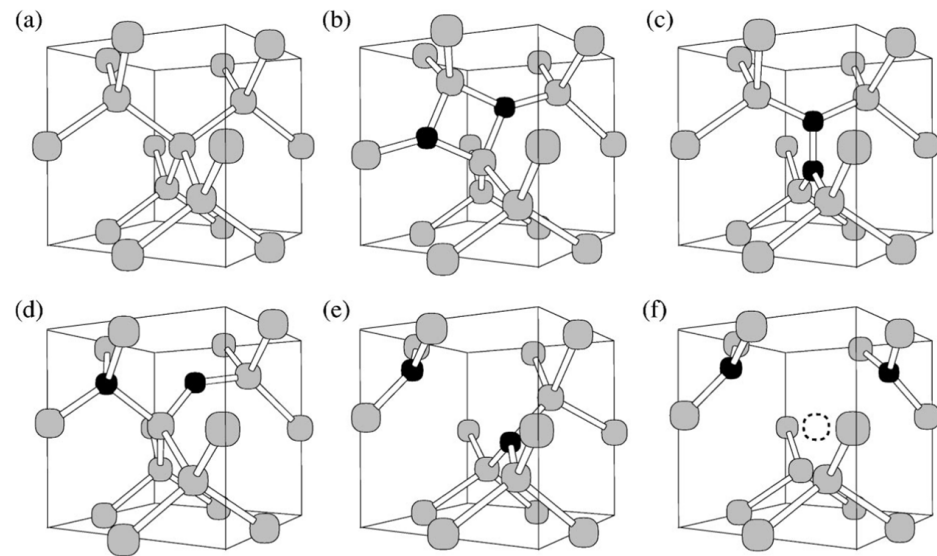### 2.2. The Nitrogen Di-Interstitial (N_iN_i) Defect

The N_i defect is mobile at around room temperature [50,63]. The diffusion of N_i in the Si lattice can lead to its association with other defects and impurities to form defect clusters. Among others, it can be readily trapped by another N_i impurity and form the nitrogen di-interstitial pair labeled as N_iN_i. It has been found that the N_iN_i pair, also labeled as the N_2 defect, is the most dominant defect of N in Si [9,64–69]. Jones et al. [64] used DFT calculations to predict that the pair consists of two neighboring <100> oriented N-Si split interstitials, arranged in an antiparallel configuration, and with the N-Si bonds forming a square lying on <011> (refer to Figure 3b). This configuration is the more stable one due to chemical and geometrical reasons [22,64,65]. Indeed, since the N atom has three valence orbitals, and the Si atom has four it is geometrically impossible to make perfect bonds between them. One valence bond will be left over. Evidently, in order to have perfect bonds two N atoms should form a pair in Si. The defect anneals out [64] at a temperature around 800 °C. Two IR active modes at 772.9 and 967.8 cm^{-1} and two Raman active modes at 743.1 and 1070.0 cm^{-1} were calculated and attributed to the N_2 defect in agreement with the experimentally [9,67] observed IR bands at 766 and 963 cm^{-1}.

2.3. The N_sV Defect

A N_s impurity can be readily associated with a vacancy to form the N_sV complex. In this structure, N_s is at a nearest neighbor site, with respect to V in the Si lattice [50,51,53,63,68,69]. The calculations of [50] predict that N_sV possesses two deep levels, one single acceptor at E_c −0.7 eV, and one double acceptor at E_c −0.5 eV. Also, an LVM band at 663 cm^{-1} was calculated [50] in association with the N_sV complex and in agreement with the experimental results [40]. The possibility was considered [63] that the defect is linked with the SL6 EPR signal [36].

In the study by Potsidi et al. [54], DFT calculations were employed to study N_sV defects in Si, with the lowest energy structure schematically represented in Figure 4a. This study confirms the formation of the N_sV defects as it is calculated that N_s and V are associate with a binding energy of −2.1 eV [54]. In the N_sV defect, the nitrogen atom effectively forms a trigonal planar structure that is distorted but has identical N-Si bond

lengths (1.84 Å) and bond angles (117.8°) (refer to Figure 4) [54]. This structure forms because of a nearest neighbor Si vacancy that alters the Si–N bond distances (~0.20 Å) as compared to the case of N_s [54]. The reason for this can be traced to the strong bonding between N and Si atoms as realized using the DFT-derived positive Bader charge analysis which shows a gain of nearly three electrons by the N atom [54]. In Figure 4c, the charge density distribution around the N and the vacancy is shown, whereas Figure 4d reveals the band-decomposed charge density [54]. Finally, the total DOS indicates that it is an n-type doped material, with the states appearing within the bandgap that is predominately associated with the nitrogen s and p electrons (refer to Figure 4e,f).

Figure 3. A schematic representation of the defects of two nitrogen atoms. (**a**) The Si lattice, (**b**) the C_{2h} N_iN_i defect, (**c**) the D_{2d} split-interstitial N_iN_s defect, (**d**) the N_s–bond-centered N_i defect, (**e**) the N_sN_s defect, and (**f**) the N_sN_sV defect. Black and gray circles represent the N and Si atoms, whereas the vacancy is indicated by a dashed circle [50].
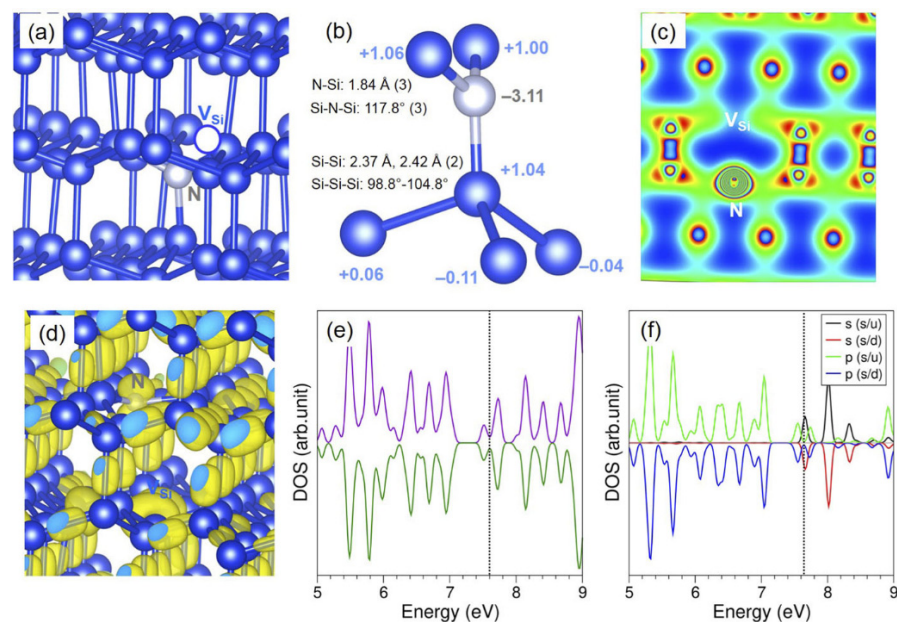
Figure 4. (**a**) The N_sV in the Si lattice, (**b**) tetrahedral units comparing Bader charges, bond distances and angles, (**c**) charge density, (**d**) band-decomposed charge density plot for the N_s, (**e**) total DOS, and (**f**) atomic DOS plot of N [54].

2.4. The N_iN_s Defect

N_i impurity is also possible to associate with a N_s atom and to form a N_iN_s defect (refer to Figure 3c,d) [50]. In essence, N_iN_s is formed when the N_iN_i defect is associated with a single-lattice V via the mechanism $N_iN_i + V \rightarrow N_iN_s$. In the structure of the N_iN_s complex, a pair of the nitrogen atoms lie at the center of the vacancy making equivalent bonds with all four Si neighbors [22,51,63,64], and calculations determine two IR active bands at around 573.4 and 774.1 cm^{-1}, which are related to the N_iN_s structure [63].

2.5. The N_sN_s Defect

The N_sN_s complex is formed when a divacancy of V_2 is trapped by a Ni -Ni defect (Ni $-N_i + V_2 \rightarrow$ (Ni $-N_i$ -V_2)) which is also labeled as N_sN_s (refer to Figure 3e) [50]. Another formation reaction that may be considered is (Ni $-$Ns $+ V \rightarrow$ (Ni N_s -V)), that is N_2V_2 [50,63]. The structure has a D_{3d} configuration. The defect was first suggested by Stein [9]. Further investigations [6,70–72] gave additional information regarding a deep level of E_c -0.42 eV, and favored correlations of their signals with complexes between nitrogen pairs and vacancies. A photoluminescence (PL) line at a photon energy of 1.1223 eV has been ascribed to a nitrogen complex in silicon. This line, which is identical to the A line of the isoelectronic A, B, C PL system, has been studied in detail previously [39,73–75] and has been tentatively correlated with the N_s $-N_s$ complex [50]. It is important to note that N_2V_2 readily interacts with O atoms leading to the formation of $N_2V_2O_n$ (n = 1, 2) complexes [53,76]. Theoretically, it has been shown that N_2V_2 has the ability to act preferentially as a nucleation site for oxygen precipitation [28,52]. More specifically, the initially formed N_2V_2 complexes capture oxygen atoms to act as heterogeneous nuclei for oxygen precipitates at high temperatures [14,77].

2.6. The $N_iN_iSi_I$ Defect

It is interesting at this point, for the sake of completion, to examine complexes when self-interstitials are added to the N_iN_i defect. The first member of the family is the $(N_iN_i)Si_I$ complex, which is also label as $(N_i)_2Si_I$ (refer to Figure 5) [50]. This structure can be thought of as a tri-self-interstitial structure [50,78] similar to that assigned to the W-photoluminescence center [79], where two of the self-interstitials were displaced by nitrogen atoms. A number of LVMs were calculated [50] (566.3, 570.4, 574.8, 810.4, 834.8, 936.2, 947.6 cm^{-1}). Experimentally, two bands at 930 and 953 cm^{-1} have been associated [45,79] with $N_iN_iSi_I$. The values of these bands compare well with the latter two theoretical values [50] at 936.2 and 747 cm^{-1}. It was predicted that the structure does not possess an acceptor level, but possess a single-donor level at around E_v $+0.2$ eV. Theoretical results [50] show that N pairs act as shallow traps for self-interstitials. Furthermore, since nitrogen affects [12,18,21] the diffusion of self-interstitials in Si, any experimental information about the $N_iN_iSi_I$ complex will deepen the understanding of the role of self-interstitials in various processes in the material.
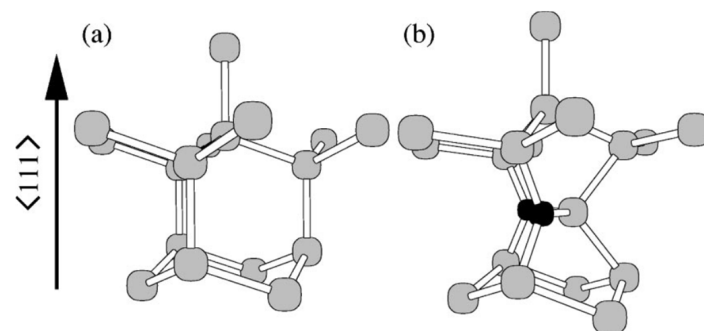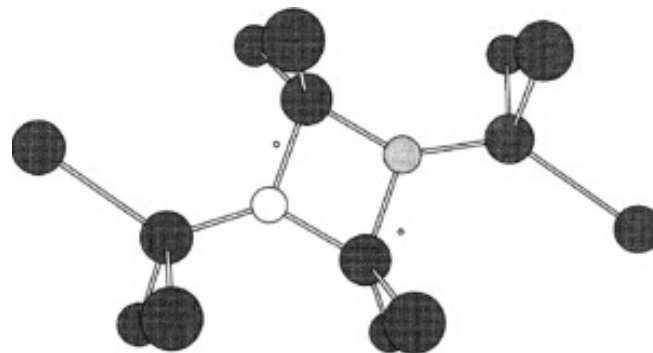

Figure 5. A schematic representation of (**a**) the Si lattice and (**b**) the $N_iN_iSi_I$ defect. Black and gray circles represent the N and Si atoms, respectively [50].

2.7. The N_sN_sV Defect

It is important also to examine complexes where vacancies are added to the N_sN_s defect. The first member of this family is the N_sN_sV complex (refer to Figure 3f). The structure was previously studied by considering [50] that both N atoms border a vacancy. The defect possesses C_{2v} symmetry and relaxes so that each of the N atoms are approximately coplanar with the three Si neighbors. The LVMs of the defect were calculated at 672, 664.9, 664.8, 662.9, and 669.1 cm^{-1}. These values are similar to those of the N_sV defects due to the fact that the N atoms in the two structures exist in similar environments [50]. Notably, the reaction $N_sN_s +V \rightarrow N_sN_sV$ has been suggested [18] to be the dominant reaction for vacancy suppression in FZ-Si. Calculations [50] show that the structure possesses a deep acceptor around E_c −0.42 eV, but further verification is needed from experimental results.
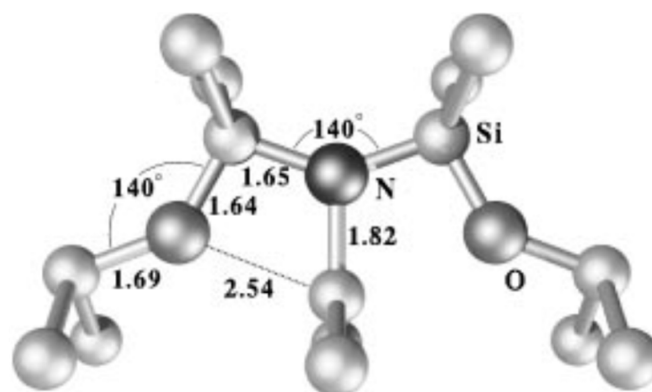
2.8. The NO Defect

N-O complexes form [14] unavoidably in CZ-Si doped with nitrogen. Theoretical calculations with the AIMPRO local density functional theory [80] found that in the neutral ground state configuration the oxygen atom is over-coordinated, that is three-fold coordinated (refer to Figure 6). In this geometry, the O and the N atoms form a square with two common silicon bonding neighbors [29,81,82]. Interestingly, in a previous study, a slightly different structure was proposed [31], where the O atom was coordinated two-fold and located in a bond-centered location. Three LVMs at 1001, 801, and 722 cm^{-1} were predicted to be related to the N-O defect [14]. Shallow thermal donors related to N-O$_x$ (x = 1 − 8) defects provide peaks [83–86] in the IR spectrum in the range ~ 190–300 cm^{-1} corresponding to transitions 1s-2p$_0$, 1s-2p$_\pm$, and 1s-3p$_\pm$. The respective values of these transitions [14] for N-O (x = 1) are 190.8, 233.8, and 260.1 cm^{-1}. Additionally, a shallow donor level at E(0/+) = E_c −0.06 eV has been linked [82] with the N-O complex.

Figure 6. A schematic representation of the NO defect. Si atoms are indicted with dark shaded circles, N with the light shaded circle, and O the empty circle. The spots represent the initial lattice positions [14].

2.9. The NO_2 Defect

The NO_2 complex has been studied theoretically, in detail, in the literature, considering two possible nearest neighbor sites for the second oxygen atom of the structure. In the first case, the two O atoms of NO_2 are situated on either side of the N atom, forming an O-N-O configuration (refer to Figure 7) [31] with a C_{2v} symmetry; although, in the second case, the two O atoms are coordinated two-fold, forming a N-O-O configuration with C_{1h} symmetry [14,81]. Notably the energy of the O-N-O is higher than that of N-O-O by about 0.2 eV [13,81]. Comparing these values with the experimentally [87] detected bands, it was suggested [81] that the bands at 855, 973, and 1002 cm^{-1} correspond to modes related to the NO_2 complex. Additionally, two other bands at 810 and 1018 cm^{-1} which have similar annealing behavior to the above three bands were also tentatively attributed [87] to the NO_2 defect. Notably, the assignment of the two latter bands has been put into question, and in particular, they have been linked [14] to the N_2O_2 defect.

Figure 7. A schematic representation of the NO_2 defect [31].

2.10. The N_2O Defect

In the N_2O structure, an O atom is trapped by a N_2 pair [88–95]. In this configuration, since the Si-Si bonds next to the (NN) ring are elongated, they can easily accommodate an interstitial oxygen atom forming a (NN)O structure (Figure 1 in [95]). The trapping of an O atom has been attributed [14] to the strain field surrounding the N_2 pair. In an alternative configuration, an additional N atom is attached in a NO defect, forming a N(NO) structure [29]. The (NN)O configuration is more stable in the neutral charge state whereas the N(NO) configuration is more stable in the positive charge state [29,30]. The experimentally determined LVMs in the middle IR at 801, 996, and 1026 cm^{-1} were attributed [9,43,88–91] to the N_2O defect. Additionally, peaks in the far IR range at 240, 242, and 249 cm^{-1} have been detected [90] and linked to electronic excitations of the N_2O defect. Notably, shallow donor levels that originated from such N-O complexes have been previously reported [92–95].

2.11. The N_2O_2 Defect

The N_2O_2 complex is formed when a N_2O structure traps an interstitial oxygen atom [14]. Two likely configurations have been discussed (refer to Figure 2 in [95]) depending on the position of the second O atom attached to the N_2O defect. In the first case, the second O atom is situated at a bond center site next to the N-pair, labeled as (ONNO); although, in the second case, the second oxygen atom is situated at a neighboring interstitial site next to the first oxygen atom, labeled as (NNOO). A number of LVMs were calculated for the N_2O_2 complex [95]. For two of them at 1003 and 813 cm^{-1}, it was suggested that they could be identified [95] with the experimentally detected lines at 1018 and 810 cm^{-1}. The two bands have been detected [87,89,96] previously and are correlated [87,96] with the NO_2 defect. However, preliminary research [95] has concluded that between the NO_2 and the N_2O_2 defects the latter is most possibly linked with the two bands, although further wok is required to verify this assignment. We notice that NNO_x ($x \geq 1$) particles have been found [97] to serve as nuclei for oxygen precipitates, although other works have reported that only NO_2 species can act [93] as nuclei for oxygen precipitates. Due to the significance of oxygen precipitates for silicon-based industries, any information about nitrogen–oxygen defects is valuable.

2.12. The $V_mN_2O_n$ (m, n = 1, 2) Defect

It has been found that it is energetically unfavorable for the N_2V_2 defect to trap further vacancies [77,98]. However, oxygen atoms can be readily captured by the N_2V_2 defect to form larger structures [14,52,53,76,99] generally labeled as $N_2V_2O_n$ (n = 1, 2) complexes, which can act as nuclei for oxygen precipitates, but also enhance the formation of oxygen precipitates [14,28,53,100,101]. The structures of the VN_2O, V_2N_2O (refer to Figure 8), VN_2O_2, and $V_2N_2O_2$ complexeshave been studied in the literature, and a number of LVMs have been correlated [14,52,56] with these structures. Certain correlations between

theoretically calculated LVMs and experimentally detected infrared lines have been made. For instance, the LVMs at 729 cm^{-1} of $V_2N_2O_2$ and the 731 cm^{-1} of V_2N_2O might be assigned [14,52] to the FTIR line at 739 cm^{-1}, which was observed experimentally [43] in nitrogen and oxygen implanted silicon. Additionally, the LVMs at 810 cm^{-1} of $V_2N_2O_2$ and 819 cm^{-1} of the V_2N_2O matches with the FTIR measured lines at 806 cm^{-1} and 815 cm^{-1} absorption lines for N-O defects [52]. Apparently, more experimental work is necessary in order for definite assignments of certain IR bands with corresponding $N_2V_2O_n$ (n = 1, 2) complexes to be established.
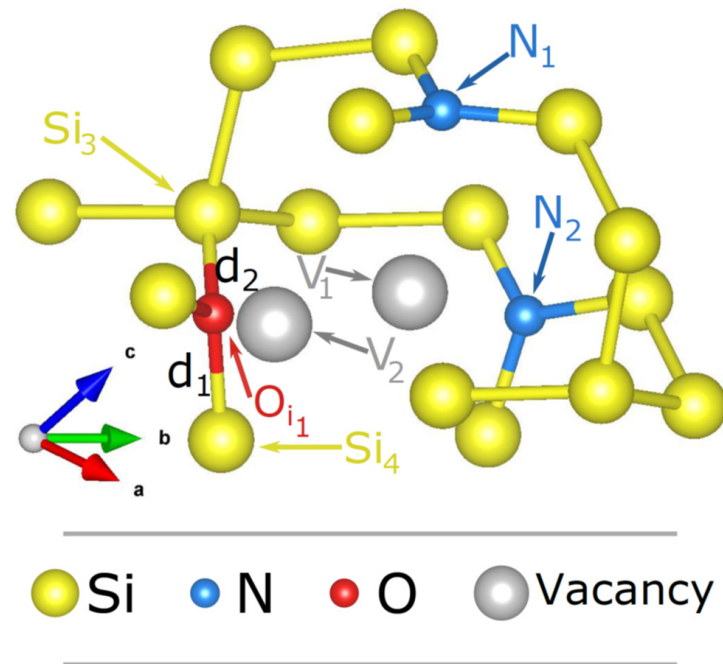
**Figure 8.** A schematic representation of the $N_2V_2O_i$ defect [56].

2.13. The CN and CNO Defects

The so-called "impurity engineering" technique is a very promising strategy to improve the quality of a material through the introduction of harmless impurities in the crystal lattice [14]. N and C are electrically neutral impurities in Si, and their presence in the lattice can improve the intrinsic gettering ability of Si; they can eliminate void defects; enhance the mechanical strength of the material; significantly affect the oxygen precipitation process; as well as reduce the size of microdefects and control their growth [14,102–104]. It deserves to be noted that optical absorption and electron spin resonance (ESR) measurements have concluded that C suppresses the formation of N-O complexes [105]. Apparently, the interaction between N and C is important in this framework, since the formation of corresponding complexes may affect the electrical and optical properties of Si. Therefore, for technological purposes any relative information about N and C-related defects is necessary for controlling Si wafers containing these impurities. Regarding the N-C pairs, systematical studies have been reported, employing the photoluminescence (PL) spectroscopy by Dormen et al. [106–109]. A number of Pl no-phonon transitions in the spectra of C and N implanted Si have been reported: N_1 = 745.6 meV, N_2 = 758.0 meV, N_3 = 761.5 meV, N_4 = 757.4 meV, and N_5 = 772.4 meV, each one with different formation temperatures. The model concluded that the N-C center involves a N atom distorted out of the substitutional lattice site along the <111> axis in an almost planar Si_3N configuration and a C_i atom, which is inserted into the N-Si bond along the <111> axis, popped out from the bond-centered position in one of the three equivalent <100> planes [106–110].

Regarding the C-N-O defect, the so-far-reported experimental results are poor. Two IR lines labeled NX_1 and NX_2 have been reported [90]. An IR line at 588 cm^{-1} labelled as

the X line of the CO complex supports the conclusion that the NX_1 and NX_2 bands may be due to a CO complex which is disturbed by a N atom in the vicinity. However, further experimental and theoretical verification is necessary.

The structures N-C and N-C-O have been recently investigated using DFT calculations [57]. The DFT results by Kuganathan et al. [57] showed that in the relaxed structure of the C_iN defect, nitrogen is in a distorted trigonal planar configuration with the nearest neighbor silicon atoms (refer to Figure 9a). The Si-N bond distances are 1.74–1.80 Å and are shorter as compared to the Si-Si bond distance (2.37 Å) in the undoped Si lattice [57]. The key is the higher electronegativity of N as compared to Si, which also impacts the Bader charges [57]. In particular, N has accumulated a high negative Bader charge (–3.21) with the nearest neighbor Si atoms having a positive Bader charge (refer to Figure 9b) [57]. Considering the C_i is tetrahedrally coordinated and has four nearest neighbor Si atoms [57]. The shorter Si-C bond distances (1.92–2.02 Å) as compared to the Si-Si bond distance and the negative Bader charge on the C atom reflect the electronegativity difference between the C and Si atoms (refer to Figure 9c) [57].
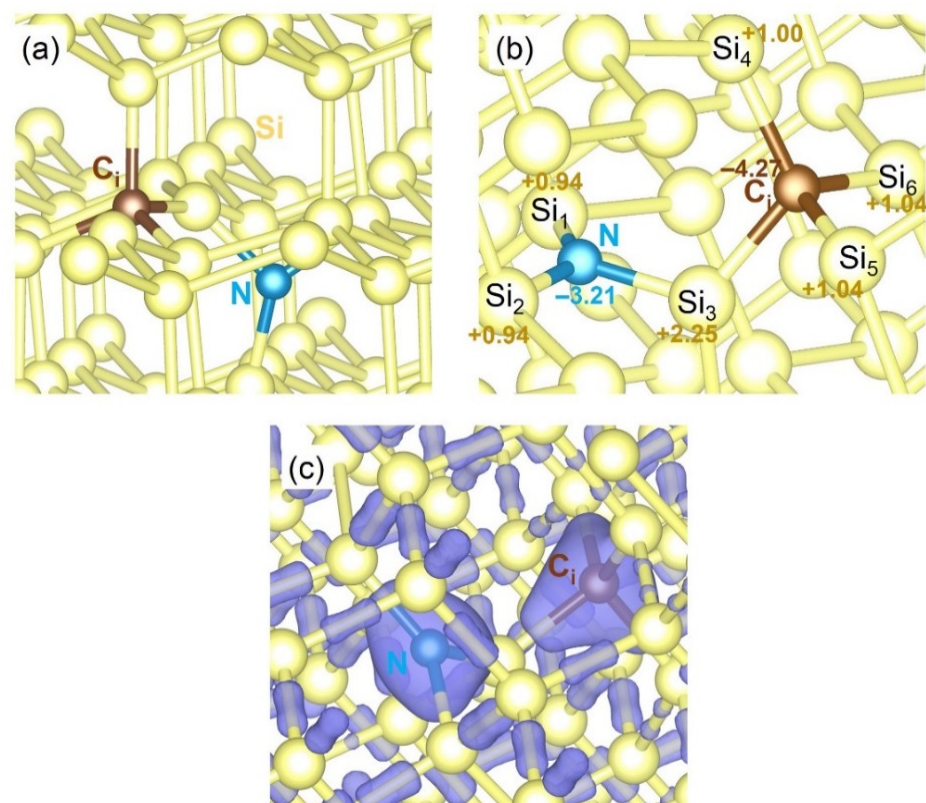
Figure 9. The C_iN defect. (**a**) The DFT relaxed structure of C_i in the presence of N-doped Si, (**b**) the Bader charges on C, N and its nearest neighbor Si atoms, and (**c**) the charge density plot representing the electron distribution around the C and N atoms [57].

The C_iNO_i defect can form by adding an O_i in the C_iN defect in Si (refer to Figure 10a) [57]. The introduction of O_i induces relatively small changes in the Bader charges, bond distances, and angles (refer to Figure 10b,c) [57]. As oxygen is more electronegative, it accumulates a Bader charge of –2.09 [57].

To aid the reader, Table 1 summarizes the properties of the most important nitrogen-containing defects in Si. These defects are also important in related materials such as Ge and group IV alloys [111,112], which are becoming increasing important in nanoelectronic devices. As such advanced computational and thermodynamic techniques will be required to investigate the intricacies of nitrogen-related defects in semiconductor alloys [113–116].
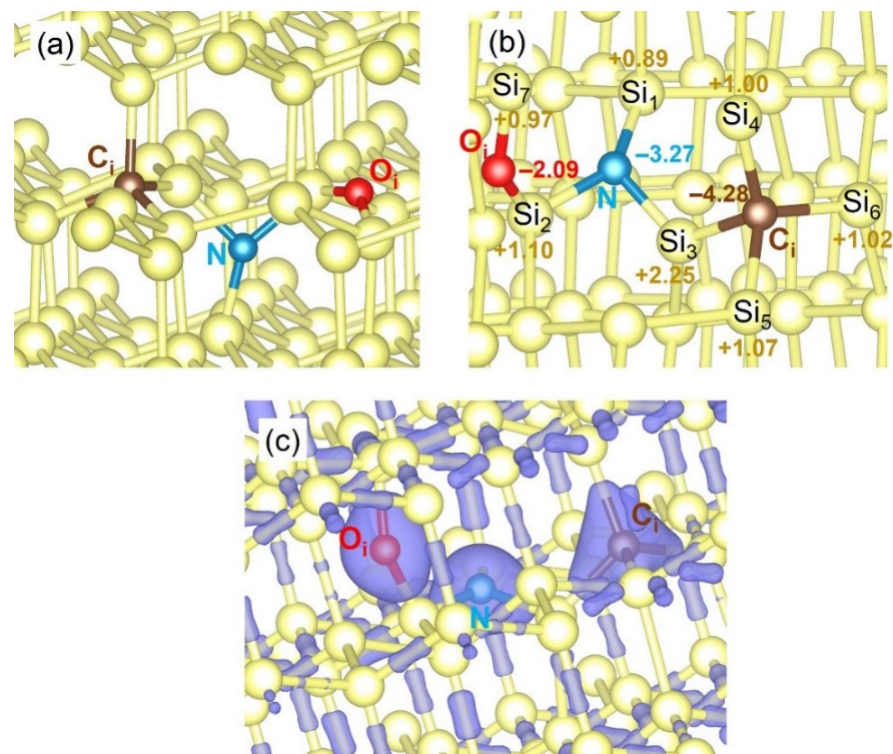
Figure 10. (**a**) The DFT relaxed structure of C_iNO_i defect in Si, (**b**) the Bader charges on C, N, O, and their nearest neighbor Si atoms, and (**c**) the charge density plot representing the electron distribution around the C, N, and O atoms [57].

Table 1. Summary of the properties of the most significant nitrogen-related defects considered.

Defect	LVM/cm^{-1}	Levels/eV	Refs.
N_s	653	$E_c-0.08$, $E_c-0.31$, $E_c-0.64$	[33,61,62]
N_i	550, 773, 885	$E_v+0.5$, $E_c-0.2$	[50,51,63]
N_iN_i	766, 963		[9,67]
N_sV	663	$E_c-0.5$, $E_c-0.7$	[50,54]
N_iN_s	573.4, 774.1		[63]
N_sN_s		$E_c-0.42$	[6,70–72]
$N_iN_iSi_I$	930, 953	$E_v+0.2$	[39,50,79]
NO	722, 801, 1001	$E_c-0.06$	[14]
NO_2	855, 973, 1002		[81,87]
N_2O	801, 996, 1026		[9,43,88–91]

3. Conclusions

In the present review, we aim to offer a comprehensive survey of nitrogen-related defects in Si. We considered both experimental and theoretical studies in order to gain a better understanding of these defects and their impact on the properties of Si. N is always present in Si, and understanding it is of fundamental importance, as the Si-related devices have reduced dimensions. In particular, it is expected that a better understanding of dopant–defect interactions involving nitrogen and/or oxygen and/or carbon and/or intrinsic defects will guide scientists/engineers to further improve the optical, electrical, and electronic properties of Si.

Institutional Review Board Statement: Not applicable.

Informed Consent Statement: Not applicable.

Data Availability Statement: Not applicable.

Conflicts of Interest: The authors declare no conflict of interest.

References

1. Dalle Betta, G.-F.; Ye, J. Silicon Radiation Detector Technologies: From planar to 3D. *Chips* **2023**, *2*, 83–101. [CrossRef]
2. Jia, X.; He, L. Noise-based analysis of the reliability of solar cells. *AIP Adv.* **2021**, *11*, 045206. [CrossRef]
3. Bisogni, M.G.; Del Guerra, A.; Belcari, N. Medical applications of silicon photomultipliers. *Nucl. Instrum. Methods Phys. Res. A* **2019**, *926*, 118–128. [CrossRef]
4. Udvarheli, P.; Somogyi, B.; Thiering, G.; Gali, A. Identification of a telecom wavelength single photon emitter in silicon. *Phys. Rev. Lett.* **2021**, *127*, 196402. [CrossRef] [PubMed]
5. Liu, W.; Ivanov, V.; Jhuria, K.; Ji, Q.; Persaud, A.; Redjem, W.; Simoni, J.; Zhiyenbayev, Y.; Kante, B.; Lopez, J.G.; et al. Quantum emitter formation dynamics and probing of radiation-induced atomic disorder in silicon. *Phys. Rev. Appl.* **2023**, *20*, 014508. [CrossRef]
6. Pichler, P. Intrinsic point defects, impurities and their diffusion in Si. In *Computational Microelectronics*; Selbercherr, S., Ed.; Springer: Vienna, Austria, 2004; pp. 378–390.
7. McCluskey, M.D.; Jannoti, A. Defects in Semiconductors. *J. Appl. Phys.* **2020**, *127*, 190401. [CrossRef]
8. Drabold, D.A.; Estreicher, S.K. (Eds.) Theory of defects in Semiconductors. In *Topics in Applied Physics*; Springer: Berlin/Heidelberg, Germany, 2007; Volume 14, pp. 1–295.
9. Stein, H.J. Nitrogen in Crystalline Silicon, in Oxygen, Carbon, Hydrogen and Nitrogen in Crystalline Silicon. In *Material Research Society Symposia Proceedings*; Mikkelsen, J.C., Jr., Pearton, S.J., Corbett, S.W., Pennycook, S.J., Eds.; Cambridge University Press: Cambridge, UK, 1986; Volume 59, pp. 523–535.
10. Habermeier, H.-U. Nitrogen in Silicon-Mechanical, Electrical and Optical properties. In *Gettering and Defect Engineering in the Semiconductor Technology*; Richter, H., Ed.; Trans Tech Publications: Stafa-Zurich, Switzerland, 1987; pp. 72–85.
11. Yang, D.; Yu, X. Nitrogen in Silicon. In *Defects and Diffusion Forum*; Trans Tech Publications: Stafa-Zurich, Switzerland, 2004; Volume 230–232, pp. 199–220.
12. Von Ammon, W.; Sattler, A.; Kissinger, G. Defects in Monocrystalline Silicon. In *Springer Handbook of Electronic and Photonic Materials*; Kasap, S., Capper, P., Eds.; Springer: Berlin/Heidelberg, Germany, 2017; pp. 111–132.
13. Yuan, S.; Yang, D. (Eds.) Nitrogen impurity in Crystalline Silicon. In *Handbook of Photovoltaic Silicon*; Springer: Berlin/ Heidelberg, Germany, 2019; pp. 463–494.
14. Yu, X.; Chen, J.; Ma, X.; Yang, D. Impurity engineering of Czochralski silicon. *Mater. Sci. Eng. R Rep.* **2013**, *74*, 1–33. [CrossRef]
15. Orlov, V.; Richter, H.; Fischer, A.; Reif, J.; Muller, T.; Wahlich, R. Mechanical properties of Nitrogen-doped CZ silicon crystals. *Mater. Sci. Semicond. Process.* **2002**, *5*, 403–407. [CrossRef]
16. Sumino, K.; Yonenaga, I.; Imai, M. Effects of nitrogen on dislocation behavior and mechanical strength in silicon crystals. *J. Appl. Phys.* **1983**, *54*, 5016–5020. [CrossRef]
17. Nakai, K.; Inoue, Y.; Yokota, H.; Ikari, A.; Takahashi, J.; Tachikawa, A.; Kitahara, K.; Ohta, Y.; Ohashi, W. Oxygen precipitation in nitrogen-doped Czochralski-grown silicon crystals. *J. Appl. Phys.* **2001**, *89*, 4301–4309. [CrossRef]
18. Von Ammon, W.; Holzi, R.; Virbulis, J.; Dornberger, E.; Schmolke, R.; Graf, D. The impact of nitrogen on the defect aggregation in silicon. *J. Cryst. Growth* **2001**, *226*, 19–30. [CrossRef]
19. Ishii, H.; Shiratake, S.; Oka, K.; Motonami, K.; Koyama, T.; Izimitani, J. Direct observation of crystal-Originated particles on Czochralski-grown silicon wafer surface and effect on gate oxide reliability. *Jpn. J. Appl. Phys.* **1996**, *35*, L1385–L1387. [CrossRef]
20. Voronkov, V.V.; Falster, R. Nitrogen interaction with vacancies in silicon. *Mater. Sci. Eng. B* **2004**, *114–115*, 130–134. [CrossRef]
21. Abe, T.; Harada, H.; Chikawa, J. Swirl defects in float-zone silicon crystals. *Phys. B Condens. Matter* **1983**, *116*, 139–147.
22. Kageshima, H.; Tagushi, A.; Wada, K. Theoretical investigation of nitrogen-doped effect on vacancy aggregation processes in Si. *Appl. Phys. Lett.* **2000**, *76*, 3718–3720. [CrossRef]
23. Kajiwara, K.; Torigoe, K.; Harada, K.; Hourai, M.; Nishizawa, S. Oxygen concentration dependence of as-grown defect formation in nitrogen-doped Czochralski silicon crystals. *J. Cryst. Growth* **2021**, *570*, 126236. [CrossRef]
24. Murthy, C.; Lee, K.; Rengarajan, R.; Dokumaci, O.; Ronsheim, P.; Tews, H.; Inaba, S. Nitrogen-induced transient enhanced diffusion of dopants. *Appl. Phys. Let.* **2002**, *80*, 2696–2698. [CrossRef]
25. Parakhonsky, A.L.; Yakimov, E.B.; Yang, D. Nitrogen effect on self-interstitial generation in Czochraski silicon revealed by gold diffusion experiments. *J. Appl. Phys.* **2001**, *90*, 3642–3644. [CrossRef]
26. Sun, C.; Lou, Z.; Ai, X.; Xue, Z.; Zhang, H.; Chen, G. Effect of nitrogen doping on pulling rate range of defect-free crystal in Cz silicon. *Coatings* **2023**, *13*, 1637. [CrossRef]
27. Cui, C.; Yang, D.; Yu, X.; Ma, X.; Li, L.; Que, D. Effect of nitrogen on denuded zone in Czochralski silicon wafer. *Semicond. Sci. Technol.* **2004**, *19*, 548–551. [CrossRef]

28. Karoui, A.; Karoui, F.S.; Rozgonyi, G.A.; Hourai, M.; Sueoka, K. Structure, energetics, and thermal stability of nitrogen-related defects in nitrogen doped silicon. *J. Electrochem. Soc.* **2003**, *150*, G771–G777. [CrossRef]

29. Gali, A.; Miro, J.; Deak, P.; Ewels, C.P.; Jones, R. Theoretical studies of nitrogen-oxygen complexes in silicon. *J. Phys. Condens. Matter* **1996**, *8*, 7711–7722. [CrossRef]

30. Jones, R.; Ewels, C.; Goss, J.; Miro, J.; Deak, P.; Osberg, S.; Rasmussen, F.B. Theoretical and isotopic infrared absorption investigations of nitrogen-oxygen defects in silicon. *Semicond. Sci. Thechnol.* **1994**, *9*, 2145–2148. [CrossRef]

31. Ewels, C.R.; Jones, R.; Osberg, S.; Miro, J.; Deak, P. Shallow thermal donors in silicon. *Phys. Rev. Lett.* **1996**, *77*, 865–868. [CrossRef]

32. Simha, C.; Herrero-Saboya, G.; Giacomazzi, L.; Martin-Samos, L.; Hemeryck, A.; Richard, N. Deep levels and electron paramagnetic resonance parameters of subsitutional nitrogen in silicon from first principles. *Nanomaterials* **2023**, *13*, 2123. [CrossRef]

33. Scheffler, L.; Lei, A.; Duum, S.; Julsgaard, B. On the nature of thermally activated defects in n-type silicon grown in nitrogen atmosphere. *AIP Adv.* **2022**, *12*, 035151. [CrossRef]

34. Nakamura, M.; Murakani, S.; Udono, H. Origins of nitrogen-related deep donor center and its preceding species in nitrogen-doped silicon determined by deep-level transient spectroscopy. *Appl. Phys. Express* **2019**, *12*, 021005. [CrossRef]

35. Kajiwara, K.; Epiguchi, K.; Fusegawa, K.; Mitsugi, N.; Samata, S.; Torigoe, K.; Harada, K.; Hourai, M.; Nishizawa, S. Evaluation of thermally activated defects behaviors in nitrogen-doped Czochralski silicon single crystals using deep level transient spestroscopy. *Jpn. J. Appl. Phys.* **2023**, *62*, 075504. [CrossRef]

36. Brower, K.L. Deep levels nitrogen centers in laser-annealed ion-implanted silicon. *Phys. Rev. B* **1982**, *26*, 6040–6052. [CrossRef]

37. Sprenger, M.; Sieverts, M.; Muller, S.H.; Ammerlaan, C.A.J. Electron paramagnetic resonance of a nitrogen-related centre in electron irradiated silicon. *Solid State Commun.* **1984**, *51*, 951–955. [CrossRef]

38. Belli, M.; Fanciulli, M.; Batani, D. Electron spin resonance of substitutional nitrogen in silicon. *Phys. Rev. B* **2014**, *89*, 115207. [CrossRef]

39. Sgourou, E.N.; Angeletos, T.; Chroneos, A.; Londos, C.A. Infrared study of defects in nitrogen-doped electron irradiated silicon. *J. Mater. Sci. Mater. Electron.* **2016**, *27*, 2054–2061. [CrossRef]

40. Potsidi, M.S.; Angeletos, T.; Londos, C.A. The origin of infrared bands in nitrogen-doped silicon. *J. Mater. Sci. Mater. Electron.* **2022**, *57*, 5507–5517.

41. Zhao, T.; Hua, C.; Lan, W.; Sun, Y.; Wu, D.; Lu, Y.; Ma, X.; Yang, D. On the mechanism underlying the elimination of nitrogen-oxygen shallow thermal donors in nitrogen-doped Czochralski silicon at elevated temperatures. *J. Appl. Phys.* **2021**, *129*, 145702. [CrossRef]

42. Stoudek, R.; Humlicek, J. Infrared spectroscopy of oxygen interstitials and precipitates in nitrogen-doped silicon. *Phys. B Condens. Matter* **2006**, *376–377*, 150–153. [CrossRef]

43. Rasmussen, F.B.; Oberg, S.; Jones, R.; Ewels, E.; Goss, J.; Miro, J.; Deak, P. The nitrogen-pair oxygen defect in silicon. *Mater. Sci. Engineer. B* **1996**, *36*, 91–95. [CrossRef]

44. Inoue, N.; Kawamura, Y. Infrared defect dynamics-nitrogen-Vacancy complexes in float zone silicon introduced by electron irradiation. *J. Appl. Phys.* **2018**, *123*, 185701. [CrossRef]

45. Tajima, M.; Masui, T.; Abe, T.; Nozaki, T. Photoluminescence associated with nitrogen in silicon. *Jpn. J. Appl. Phys.* **1981**, *20*, L423–L425. [CrossRef]

46. Steele, A.G.; Lenchyshyn, L.C.; Thewalt, M.L.W. Photoluminescence study of nitrogen-oxygen donors in silicon. *Appl. Phys. Lett.* **1990**, *56*, 148–150. [CrossRef]

47. Surma, B.; Misiuk, A.; Wnuk, A.; Bukowski, A.; Rzodkiewicz, W. Photoluminescence studies of defects created in nitrogen-doped silicon during annealing under enhanced pressure. *Mater. Sci. Semicond. Process.* **2004**, *7*, 404–409. [CrossRef]

48. Platonenko, A.; Gentile, F.S.; Pascale, F.; Ferrari, A.M.; D'Amore, M.; Dovesi, R. Nitrogen substitutional defects in silicon. A quantum mechanical investigation of the structural, electronic and vibrational properties. *Phys. Chem. Chem. Phys.* **2019**, *21*, 20939. [CrossRef]

49. Platonenko, A.; Gentile, F.S.; Maul, J.; Pascale, F.; Kotomin, E.A.; Dovesi, R. Nitrogen interstitial defects in silicon. A quantum mechanical investigation of the structural, electronic and vibrational properties. *Mater. Today Commun.* **2019**, *21*, 100616. [CrossRef]

50. Goss, J.P.; Hahm, I.; Jones, R.; Briddon, P.R.; Oberg, S. Vibrational modes and electronic properties of nitrogen defects in silicon. *Phys. Rev. B* **2003**, *67*, 045206. [CrossRef]

51. Sawada, H.; Kawakami, K. First-principles calculation of the interaction between nitrogen atoms and vacancies in silicon. *Phys. Rev. B* **2000**, *62*, 1851–1858. [CrossRef]

52. Karoui, F.S.; Karoui, A. A density functional theory study of the atomic structure, formation energy and vibrational properties of nitrogen-vacancy-oxygen defects in silicon. *J. Appl. Phys.* **2010**, *108*, 033513. [CrossRef]

53. Kageshima, H.; Taguchi, A.; Wada, K. Formation of stable N-V-O complexes in Si. *Phys. B Condens. Matter* **2003**, *340–342*, 626–629. [CrossRef]

54. Potsidi, M.S.; Kuganathan, N.; Christopoulos, S.-R.G.; Sarlis, N.V.; Chroneos, A.; Londos, C.A. Theoretical investigation of nitrogen-vacancy defects in silicon. *AIP Adv.* **2022**, *12*, 025112. [CrossRef]

55. Papadopoulou, K.A.; Chroneos, A.; Christopoulos, S.-R.G. The $(N_s)_2(O_i)_n$ (n = 1, 2) defect in Si from Density Functional theory perspective. *Phys. B Condens. Matter* **2022**, *643*, 414184. [CrossRef]

56. Christopoulos, S.-R.G.; Sgourou, E.N.; Chroneos, A.; Londos, C.A. Density functional theory study of the $V_mN_2O_n$ (m, n = 1, 2) complexes in silicon. *Mod. Phys. Lett. B* **2023**, *14*, 2350035. [CrossRef]

57. Kuganathan, N.; Christopoulos, S.-R.G.; Papadopoulou, K.A.; Sgourou, E.N.; Chroneos, A.; Londos, C.A. A density functional theory study of the C_iN and C_iNO_i complexes in silicon. *Mod. Phys. Lett. B* **2023**, *14*, 2350154. [CrossRef]

58. Brower, K.L. Jahn-Teller-distorted Nitrogen donor in laser-annealed silicon. *Phys. Rev. Lett.* **1980**, *44*, 1627–1629. [CrossRef]

59. Murakami, K.; Kuribayashi, H.; Masuda, K. Electronic energy levels of off-center substitutional nitrogen in silicon: Determination by electron spin resonance measurements. *Jpn. J. Appl. Phys.* **1988**, *27*, L1414–L1416. [CrossRef]

60. Murakami, K.; Kuribayashi, H.; Masuda, K. Motional effects between on-center and off-center substitutional nitrogen in silicon. *Phys. Rev. B* **1988**, *38*, 1589–1592. [CrossRef]

61. Stein, H.J. Infrared absorption band of substitutional nitrogen in silicon. *Appl. Phys. Lett.* **1985**, *47*, 1339–1341. [CrossRef]

62. Itoh, H.; Murakami, K.; Takita, K.; Masuda, K. Charge-state changes of substitutional nitrogen impurities in silicon induced by additional impurities and defects. *J. Appl. Phys.* **1987**, *61*, 4862–4868. [CrossRef]

63. Jones, R.; Hahm, I.; Goss, J.P.; Briddon, P.R.; Oberg, S. Structure and electronic properties of nitrogen defects in silicon. *Solid State Phenom.* **2004**, *95–96*, 93–98. [CrossRef]

64. Jones, R.; Oberg, S.; Rasmussen, F.B.; Nielsen, B.B. Identification of the dominant nitrogen defect in silicon. *Phys. Rev. Lett.* **1994**, *72*, 1882–1885. [CrossRef]

65. Rasmussen, F.B.; Nielsen, B.B. Microstructure of the nitrogen pair in crystalline silicon by ion channeling. *Phys. Rev. B* **1994**, *49*, 16353–16360. [CrossRef] [PubMed]

66. Stein, H.J. Evidence of pairing of implanted nitrogen in silicon. In Proceedings of the 13th International Conference on Defects in Semiconductors, Coronado, CA, USA, 12–17 August 1984; The Metallurgical Society of AIME: Warrendale, PA, USA, 1985; pp. 839–845.

67. Rasmussen, F.B.; Nielsen, B.B.; Jones, R.; Oberg, S. The nitrogen pair in crystalline silicon studied by ion channeling. *Mater. Sci. Forum* **1994**, *143–147*, 1221–1226. [CrossRef] [PubMed]

68. Nelson, J.S.; Schultz, P.A.; Wright, A.F. Valence and atomic size dependent exchange barriers in vacancy-mediated dopant diffusion. *Appl. Phys. Let.* **1998**, *73*, 247–249. [CrossRef]

69. Adam, L.S.; Law, M.E.; Szpala, S.S.; Simpson, R.J.; Lawther, D.; Documaci, O.; Hegde, S. Experimental identification of nitrogen-vacancy complexes in nitrogen implanted silicon. *Appl. Phys. Lett.* **2001**, *79*, 623–625. [CrossRef]

70. Abe, T.; Harada, H.; Ozawa, N.; Adomi, K. Deep level generation—Annihilation in nitrogen doped FZ crystals. In Proceedings of the Oxygen, Carbon, Hydrogen and Nitrogen in Crystalline Silicon, Boston, MA, USA, 2–5 December 1985.

71. Fuma, N.; Tashiro, K.; Kamumoto, K.; Takano, Y. Generation of deep Level by nitrogen diffusion in Si. *Mater. Sci. Forum* **1995**, *196–201*, 797–802. [CrossRef]

72. Fuma, N.; Tashiro, K.; Kamumoto, K.; Takano, Y. Diffused nitrogen-related deep level in n-type silicon. *Jpn. J. Appl. Phys. Part 1* **1996**, *35*, 1993–1999. [CrossRef]

73. Sauer, R.; Weber, J.; Zulehner, W. Nitrogen in silicon: Towards the identification of the 1.1223-eV (A, B, C) photoluminescence lines. *Appl. Phys. Lett.* **1984**, *44*, 440–442. [CrossRef]

74. Alt, H.C.; Tapfer, L. Photoluminescence study of nitrogen implanted silicon. *Appl. Phys. Lett.* **1984**, *45*, 426–428. [CrossRef]

75. Davies, G.; Iqbal, M.Z.; Lightowlers, E.C. Exciton self-trapping at an isoelectronic center in silicon. *Phys. Rev. B* **1994**, *50*, 11520–11530. [CrossRef] [PubMed]

76. Karoui, A.; Rozgonyi, G.A. Oxygen precipitation in nitrogen doped Czochralski silicon wafers. II. Effects of nitrogen and oxygen coupling. *J. Appl. Phys.* **2004**, *96*, 3264–3271. [CrossRef]

77. Yu, X.; Yang, D.; Ma, X.; Yang, J.; Li, L.; Que, D. Grown-in defects in nitrogen-doped Czochralski silicon. *J. Appl. Phys.* **2002**, *92*, 188–194. [CrossRef]

78. Kageshima, H.; Taguchi, A.; Wada, K. *Theoretical Investigation of Nitrogen-Doping Effect on Native Defect Aggregation Processes in Silicon*; Cambridge University Press: Cambridge, UK, 2011.

79. Coomer, B.J.; Goss, J.P.; Jones, R.; Oberg, S.; Briddon, P.R. Interstitial aggregates and a new model for the I_1/W optical center in silicon. *Phys. B Condens. Matter* **1999**, *273–274*, 505–508. [CrossRef]

80. Briddon, P.R.; Jones, R. LDA calculations using a basis of gaussian orbitals. *Phys. Stat. Sol. B* **2000**, *217*, 131–171. [CrossRef]

81. Fujita, N.; Jones, R.; Oberg, S.; Briddon, P.R. First-principles study on the local vibrational modes of nitrogen oxygen defects in silicon. *Phys. B Condens. Matter* **2007**, *401–402*, 159–162. [CrossRef]

82. Fujita, N.; Jones, R.; Oberg, S.; Briddon, P.R. Nitrogen related shallow thermal donors in silicon. *Appl. Phys. Lett.* **2007**, *91*, 051914. [CrossRef]

83. Yang, D.; Fan, R.; Li, L.; Que, D. Effect of nitrogen oxygen complex on electrical properties of Czochralski silicon. *Appl. Phys. Lett.* **1996**, *68*, 487–489. [CrossRef]

84. Alt, H.C.; Gemeniuk, Y.V.; Bittersberger, F.; Kempf, A.; Zemke, D. Analysis of electrically active N–O complexes in nitrogen-doped CZ silicon crystals by FTIR spectroscopy. *Mater. Sci. Semicond. Proc.* **2006**, *9*, 114–116. [CrossRef]

85. Suezawa, M.; Sumino, K.; Harada, H.; Abe, T. The nature of nitrogen-oxygen complexes in silicon. *Jpn. J. Appl. Phys.* **1988**, *27*, 62–67. [CrossRef]

86. Suezawa, M.; Sumino, K.; Harada, H.; Abe, T. Nitrogen-Oxygen complexes as shallow donor in silicon crystals. *Jpn. J. Appl. Phys.* **1986**, *25*, L859–L861. [CrossRef]

87. Inoue, N.; Nakatsu, M.; Tanahashi, K.; Yamada-Kaneta, H.; Ono, H.; Akhmetov, V.D.; Lysytskiy, O.; Richter, H. Annealing behavior of new nitrogen infrared absorption peaks in CZS silicon. *Solid State Phenom.* **2005**, *108–109*, 609–614. [CrossRef]

88. Wagner, P.; Oeder, R.; Zulehner, W. Nitrogen-Oxygen complexes in Czochralski-silicon. *Appl. Phys. A* **1998**, *46*, 73–76. [CrossRef]

89. Yang, D.; Que, D.; Sumino, K. Nitrogen-Oxygen complexes in silicon. *Phys. Stat. Sol. B* **1998**, *210*, 295–299. [CrossRef]

90. Yang, D.; Ma, X.; Fan, R.; Li, D.; Zhang, J.; Li, L.; Que, D.; Sumino, K. Infrared absorption of nitrogen-oxygen complex in silicon. *Mat. Sci. Eng.* **2000**, *B72*, 121–123. [CrossRef]

91. Qi, M.W.; Tan, S.S.; Zhu, B.; Cai, P.X.; Gu, W.F.; Xu, X.M.; Shi, T.S.; Que, D.L.; Li, L.B. The evidence for interaction of N-N pair with oxygen in Czochralski silicon. *J. Appl. Phys.* **1991**, *69*, 3775–3777. [CrossRef]

92. Suezawa, M.; Sumino, K. Nitrogen-Oxygen complexes in silicon. In *Defects in Electronic Materials, Material Research Society Symposia Proceedings*; Stavola, M., Pearton, S.J., Davies, G., Eds.; Cambridge University Press: Cambridge, UK, 1988; Volume 104, pp. 193–196.

93. Ono, H.; Horikawa, M. Qualitative detection of small amounts of nitrogen in Czochralski silicon crystals. *Jpn. J. Appl. Phys.* **2003**, *42*, L261–L263. [CrossRef]

94. Wagner, H.E.; Alt, H.C.; von Ammon, W.; Bittersberger, F.; Huber, A.; Koester, L. N-O related shallow donors in silicon: Stoichiometry investigations. *Appl. Phys. Lett.* **2007**, *91*, 152102. [CrossRef]

95. Fujita, N.; Jones, R.; Oberg, S.; Briddon, P.R. Local vibrational modes of N_2-O_n defects in Cz-silicon. *J. Mater. Sci. Mater. Electron.* **2007**, *18*, 683–687. [CrossRef]

96. Inoue, N.; Nakatsu, M.; Ono, H. Local vibrational modes of shallow thermal donors in nitrogen-doped Cz silicon crystals. *Phys. B Condens. Matter* **2006**, *376–377*, 101–104. [CrossRef]

97. Li, M.; Yang, D.; Ma, X.; Cui, C.; Que, D. Evolution of nitrogen pairs and nitrogen-oxygen complexes in nitrogen-doped Czochralski silicon. *Phys. Stat. Sol. C* **2007**, *4*, 3090–3094. [CrossRef]

98. Yamanaka, Y.; Harada, H.; Takahashi, K.; Mikayama, T.; Inoue, N. Infrared absorption analysis of nitrogen in Czochralski silicon. *Solid State Phenom.* **2002**, *82–84*, 69–74. [CrossRef]

99. Cui, C.; Ma, X.; Yang, D. Enhancing oxygen precipitation in neutron-irradiated nitrogen-doped Czochrakski silicon crystals. *J. Appl. Phys.* **2008**, *104*, 123523. [CrossRef]

100. Karoui, A.; Karoui, F.S.; Rozgonyi, G.A.; Hourai, M.; Sueoka, K. Characterization of nucleation sites in nitrogen doped Czochralski silicon by density functional and molecular mechanics. *Solid State Phenom.* **2004**, *95–96*, 99–104.

101. Sada, A.; Noda, Y.; Sueoka, K.; Kajiwara, K.; Hourai, M. First principle analysis on void-reduction mechanism and the impact of oxygen in nitrogen-doped CZ-Si crystal. *J. Cryst. Growth* **2023**, *610*, 127176. [CrossRef]

102. Chen, J.; Ma, X.; Yang, D. Impurity engineering in Czochralski silicon. *Solid State Phenom.* **2010**, *156–158*, 261–267. [CrossRef]

103. Sun, Q.; Yao, K.H.; Gatos, H.C. Effects of nitrogen on oxygen precipitation in silicon. *J. Appl. Phys.* **1992**, *71*, 3760–3765. [CrossRef]

104. Takahashi, J.; Nakai, K.; Kawakami, K.; Inoue, Y.; Yokota, H.; Tachikawa, A.; Ikari, A.; Ohashi, W. Microvoid defects in nitrogen–and /or carbon-doped Czochralski-grown silicon crystals. *Jpn. J. Appl. Phys.* **2003**, *42*, 363–370. [CrossRef]

105. Hara, A.; Ohsawa, A. New carbon related defects formed in nitrogen rich Czochralski silicon crystals. *Appl. Phys. Lett.* **1991**, *59*, 1890–1892. [CrossRef]

106. Dormen, A.; Pensl, G.; Sauer, R. Nitrogen-carbon radiative defect at 0.746 eV in silicon. *Phys. Rev. B* **1986**, *33*, 1495–1498. [CrossRef] [PubMed]

107. Dormen, A.; Pensl, G.; Sauer, R. Set of five related photoluminescence defects in silicon formed through nitrogen-carbon interactions. *Phys. Rev. B* **1987**, *35*, 9318–9321. [CrossRef] [PubMed]

108. Dormen, A.; Sauer, R.; Pensl, G. Nitrogen-carbon interactions in optical defects in silicon. In *Material Research Society Symposia Proceedings*; Mikkelsen, J.C., Jr., Pearton, S.J., Corbett, S.W., Pennycook, S.J., Eds.; Springer: Berlin/Heidelberg, Germany, 1986; Volume 59, pp. 523–535.

109. Dormen, A.; Sauer, R.; Pensl, G. Vibrational mode nitrogen and carbon isotope shifts on the N_1 (0.746 eV) photoluminescence spectrum in silicon. *Solid State Commun.* **1986**, *57*, 861–864. [CrossRef]

110. Dormen, A.; Sauer, R.; Pensl, G. Complexing of nitrogen with carbon and oxygen in silicon: Photoluminescence studies. *J. Elect. Mater.* **1988**, *17*, 121–125. [CrossRef]

111. Chroneos, A.; Jiang, C.; Grimes, R.W.; Schwingenschlögl, U.; Bracht, H. E centers in $Si_{1-x-y}Ge_xSn_y$ alloys. *Appl. Phys. Lett.* **2009**, *95*, 112101. [CrossRef]

112. Chroneos, A.; Sgourou, E.N.; Londos, C.A.; Schwingenschlögl, U. Oxygen defect processes in silicon and silicon germanium. *Appl. Phys. Rev.* **2015**, *2*, 021306. [CrossRef]

113. Varotsos, P. Point defect parameters in β-PbF_2 revisited. *Solid State Ion.* **2008**, *179*, 438–441. [CrossRef]

114. Zhang, B.; Wu, X.; Xu, J.; Zhou, R. Application of the cBΩ model for the calculation of oxygen self-diffusion coefficients in minerals. *J. Appl. Phys.* **2010**, *108*, 053505. [CrossRef]

115. Vallianatos, F.; Saltas, V. Application of the *cB*Ω model to the calculation of diffusion parameters of He in olivine. *Phys. Chem. Miner.* **2014**, *41*, 181–188. [CrossRef]

116. Cooper, M.W.D.; Grimes, R.W.; Fitzpatrick, M.E.; Chroneos, A. Modeling oxygen self-diffusion in UO_2 under pressure. *Solid State Ion.* **2015**, *282*, 26–30. [CrossRef]